The Physics of Metals and Metallography, Vol. 83, No. 5, 1997, pp. 461–467.

THEORY OF METALS

Calculation of Electronic Properties of Paramagnetic Cu–Ni Alloys Using APW Method in the Virtual-Crystal Approximation

A. S. Karolik and V. M. Golub

Institute of Applied Physics, Belarussian Academy of Sciences, ul. Skoriny 16, Minsk, 220072 Belarus

Received August 2, 1995; in final form, August 15, 1996

Abstract—The density of electron states, electronic heat capacity $\gamma(x)$, and the coefficient of absolute electron-diffusion thermoelectric power $S(x)$ were calculated as functions of concentration for disordered paramagnetic $Cu_{1-x}Ni_x$ alloys in the Schoen's virtual-crystal approximation using the augmented-plane-wave method. The calculations were performed over the whole concentration range at 0.1 intervals. The non-self-consistent muffin-tin potential was constructed based on the Rothaan–Hartree–Fock atomic wave functions and contained an exchange correction that satisfied the virial theorem. The calculated results are compared with experimental data.

INTRODUCTION

Copper–nickel alloys have attracted the attention of scientists for more than fifty years. The complete mutual solubility, the absence of structural and phase transformations (except for ferromagnetic ordering), and the same type of crystal lattice favor their usage for testing different theoretical models of alloying. The first attempts at explaining the properties of these alloys were made based on the rigid-band model [1]. Within this model, many of physical properties (the concentration dependence of magnetic susceptibility, Curie temperature, Hall coefficient, etc.) were explained qualitatively. The interpretation was most successful for high nickel contents [1, 2]. However, a number of other properties, e.g., photoemission spectra, changes in the parameters of Fermi surfaces, and thermoelectric properties, disagreed with the predictions of this model. The most progress in explaining and calculating physical properties of nickel–copper as well as other disordered alloys was achieved using the coherent-potential approximation (CPA) [3–7]. Presently, this self-consistent approximation based on the theory of multiple scattering is extensively and successfully used in different methods of band-structure calculations (SCF, KKR, LMTO, LCAO, etc.). Yet, despite considerable advances in calculations of electron energy spectra, optical properties, and parameters of Fermi surfaces, the calculated physical properties are not always in good agreement with the experimental data, especially at low contents of a transition element. An additional disadvantage of CPA, especially of its earliest versions [3, 4], is a strong dependence of the results on the choice of the scattering parameter δ that describes the energy spacing between the d resonances of the components.

The thermoelectric power of a metal is highly sensitive to the presence of impurities in it. Currently, the effects of impurities on the thermopower are adequately calculated only for small impurity contents less than 1 at. % and, generally, for simple-metal hosts [8, 9]. These calculations usually involve computations of characteristic thermopowers of impurities. They are valid for the concentration ranges in which the impurities either do not change the electronic structure of the solvent metal or form a dilute magnetic solution with virtual bound states described by the Kondo theory or the Anderson model. For more concentrated solid solutions, it is possible, presently, either to qualitatively describe the thermoelectric properties [10, 11] or to achieve quantitative agreement with experimental data in a limited range of concentrations using adjustable parameters or *a priori* known experimental dependences of other properties [12, 13]. Generally, the results of *ab initio* calculations are not only in poor quantitative agreement with the experimental data, but also show a different behavior [14, 15]. For copper–nickel alloys, no calculations of this type were performed for a broad concentration range.

In this paper, we made an attempt to perform such calculations. For calculating the electron energy spectrum of disordered paramagnetic Cu–Ni alloys, we used the augmented-plane-wave method and the virtual-crystal approximation (APW–VCA) [16]. In contrast to the earlier model of virtual crystal (VCM) [17], in which the alloy was replaced by a single-component crystal with an averaged potential, the virtual-crystal approximation reveals the individual features of spectra of alloy components owing to the construction of a multicomponent muffin-tin potential of the alloy. Another difference is that the VCM is only applicable when the components have sufficiently close potentials and sufficiently broad bands, whereas VCA may be used for alloys with arbitrary components. When used

within one of the most exact methods for calculating band structure, the APW–VCA method allows *ab initio* calculations of the spectra and physical properties. The disadvantage of this method is the large body of computations required to ensure self-consistency, which is one of the reasons why it is relatively rarely used. Most extensively, the APW–VCA method was used for calculating the electron energy spectra and properties of nonstoichiometric compounds. We are unaware of any application of this method to calculations in a broad concentration range, including the transition metal–noble metal alloys.

Below, we present the results of non-self-consistent APW–VCA calculation for the density of electron states, the temperature coefficient of electronic heat capacity, and the diffusion thermopower. The initial approximation used in these calculations was previously tested by us in calculating the energy spectra and properties of pure Cu, Ni, Ag, and Pd [18].

THERMOELECTRIC POWER OF TRANSITION METAL–NOBLE METAL ALLOYS

The early attempts of explaining the thermoelectric properties of alloys of transition metals with noble metals (Cu, Ag, Au) were based on the rigid-band model [1, 2]. This model provided a reasonably adequate description of thermoelectric power only for high concentrations of the transition component, at which the univalent impurity produces only a slight perturbation. When dissolved in a noble metal, even a small amount of transition-element impurity causes a strong perturbation in the energy spectrum of solvent metal, forming an additional *d* subband with a relatively high density of states near the Fermi level. The height of the additional *d* peak increases with increasing concentration of transition component.

Because the thermopower S reverses its sign on adding only a few fractions of atomic percent of transition element to the noble-metal host, it may be inferred that even at a low content of transition *d* impurity (a fraction of atomic percent and higher), the perturbation caused by the transition impurity is so large that the transport properties of these alloys may be interpreted in terms of the Mott theory [1]. According to this theory, in metals in which the *s* band with a low density of states overlaps an almost filled *d* band with a high density of states, the principal mechanism of *s* electron scattering is the scattering into the empty states of the *d* band.

Because the *d* electrons are more tightly bound to the atoms and are less mobile, so that their effective mass and conductivity obey the relationships $m_d^* \gg m_s^*$ and $\sigma_d \ll \sigma_s$, the expression for the thermopower of a two-band conductor

$$S = \frac{\sigma_s S_s + \sigma_d S_d}{\sigma_s + \sigma_d} \qquad (1)$$

reduces to the expression [8]

$$S = S_s = -\frac{\pi^2 k_B^2 T}{3|e|}\left(\frac{d\ln\sigma_s}{dE}\right)_{E=E_F}, \qquad (2)$$

where S_s, S_d, σ_s, and σ_d are the partial thermopowers and conductivities of the *s* and *d* bands, respectively. As the densities of states obey the relationship $N_d \gg N_s$ and *s–d* scattering dominates over the *s–s* scattering, so that the corresponding relaxation times satisfy the inequality $\tau_{ss}^{-1} \ll \tau_{sd}^{-1}$ and $\tau_{sd}^{-1} \sim N_d$, the thermopower may be represented in the form

$$S = \frac{\pi^2 k_B^2 T}{3|e|E_F}\left[\frac{d\ln N_d}{d\ln E} - \frac{d\ln(vF)}{d\ln E}\right]_{E_F}, \qquad (3)$$

where v is the velocity of conduction electrons, and F is the area of the Fermi surface.

Our preliminary estimates showed [18] that the second bracketed term does not exceed 3/2 for Cu–Ni alloys, whereas at concentrations above 10 at. %, the first term is at least an order of magnitude larger in absolute value and determines the thermoelectric properties of the alloys. Hence, the thermopower of these alloys may be reasonably well approximated by the expression

$$S = \frac{\pi^2 k_B^2 T}{3|e|}\frac{1}{N(E_F)}\left(\frac{dN}{dE}\right)_{E_F}. \qquad (4)$$

Based on this expression, the authors of [19] gave a semiquantitative explanation of the concentration dependence of absolute and hydrostatic-pressure-induced thermoelectric powers in Cu–Ni alloys in the whole concentration range. In this paper, these theoretical concepts were used for exact calculations of concentration-dependent electronic properties of these alloys.

CALCULATION METHOD AND RESULTS

For calculating the density of states in disordered paramagnetic copper–nickel alloys, we used the virtual-crystal approximation developed by Schoen within the augmented-plane-wave method for substitutionally disordered solid solutions and nonstoichiometric compounds [16] (APW–VCA). The crystal potential was constructed using the Mattheiss method with Coulomb and exchange components calculated separately. As the initial approximation for constructing the muffin-tin potential, we used the self-consistent Rothaan–Hartree–Fock atomic wave functions [20], which are conveniently presented in the analytic form unlike the Hartree–Fock, Hartree–Fock–Slater, and Dirac wave functions most frequently used in band calculations. The coefficients of the potential were assumed to be linear

functions of concentration. The Coulomb component of the potential is of the form

$$V_c(\mathbf{r}) = V_k(\mathbf{r}) + \sum_t n_t \sum_\eta c_{\eta t} V_\eta(R_t, \mathbf{r}), \quad (5)$$

where $V_k(\mathbf{r})$ is the Coulomb potential of the central atom of type k, $V_\eta(R_t, \mathbf{r})$ is the Coulomb contribution from atom η of the neighboring shell t, R_t is the radius of shell t, n_t is the number of atoms in this shell, and $c_{\eta t}$ is the partial concentration of component η.

The exchange potential was constructed in the Slater X_α approximation:

$$V_x(\mathbf{r}) = -a6\left\{\frac{3}{8\pi}\left[\rho_k(\mathbf{r}) + \sum_t n_t \sum_{\eta=1}^{2} c_{\eta t}\rho_\eta(R_t, \mathbf{r})\right]\right\}, \quad (6)$$

where $\rho_k(\mathbf{r})$ is the electron density at the central atom and $\rho_\eta(R_t, \mathbf{r})$ is the contribution to the electron density from the atom of type η of the neighboring shell t. The exchange correction α for pure component metals was chosen so as to satisfy the virial theorem; namely, it was 0.70635 and 0.70843 for copper and nickel, respectively [21]. This choice of parameter α allows taking into account both exchange and correlation effects because, in this case, it may be considered as the average of $\alpha(\mathbf{r})$ taken over the atomic sphere. The parameter α for the alloy was assumed to be a linear function of concentration. The value of the constant potential between the muffin-tin spheres, V_c, was obtained by averaging it over the interval between the radius of the muffin-tin sphere and the radius of the cell equivalent to the Wigner–Seitz cell. Both these quantities depend on the lattice parameter of the alloy a, which is also assumed to be a linear function of concentration

$$a = xa_{\mathrm{Ni}} + (1-x)a_{\mathrm{Cu}},$$

where a_{Ni} and a_{Cu} are the lattice parameters of components, and x is the relative concentration of nickel in the alloy.

The Schrödinger equation was solved using the augmented-plane-wave method [22]. The matrix elements H_{ij} are of the form similar to their traditional representation in the APW method but modified by the presence of η components in the alloy. For a unit cell containing s atoms, they may be written in the form

$$H_{ij} = (\mathbf{k}_i\mathbf{k}_j - E)\delta_{ij} - \sum_s \frac{4\pi(R_{MT}^s)^2}{\Omega_0}\exp(ik_{ij}r_s)F_{ij,s}, \quad (7)$$

where

$$F_{ij,s} = (\mathbf{k}_i\mathbf{k}_j - E)j_l(k_{ij}R_{MT}^s)/k_{ij} - \sum_l (2l+1)P_l(\cos\theta_{ij}) \times j_l(k_iR_{MT}^s)j_l(k_jR_{MT}^s)\sum_\eta C_{\eta s}L_l^\eta(E, R_{MT}^s),$$

$\mathbf{k}_i = \mathbf{k} + \mathbf{K}_i$, $\mathbf{k}_{ij} = \mathbf{K}_i - \mathbf{K}_j$, $\mathbf{K}_i$ is the vector of the reciprocal lattice, Ω_0 is the volume of unit cell, $\mathbf{r}_s$ is the vector connecting the center of the cell and site s of the cell, R_{MT} is the radius of the muffin-tin sphere, j_l are the Bessel functions, P_l are Legendre polynomials, θ_{ij} is the angle between the vectors $(\mathbf{k} + \mathbf{K}_i)$ and $(\mathbf{k} + \mathbf{K}_j)$, and L_l^η is the logarithmic derivative of the radial component of wave function l at the surface of the muffin-tin sphere. In calculations, we used 27 basis APWs, and the summation over l was performed up to $l = 12$. The integration over the Brillouin zone was performed using the tetrahedron method [21]. The Fermi energy E_F was determined by integrating the total density of states and equating it to the number of conduction electrons per atom, $n = 11 - x$.

Because of cumbersome and highly time-consuming computations, the self-consistency procedure for the potential was not realized, which, however, is quite admissible provided that the initial approximation is appropriately chosen [21, 22]. The initial approximation for the potential used in this paper was previously tested in APW calculations of electron energy spectra and properties of pure component metals [18]. The calculated energy spectra, characteristic energy intervals, and parameters of the Fermi surface were in good or at least reasonable agreement with the existing experimental data and the results of self-consistent calculations performed by APW and other methods.

In this paper, we used the same electron configurations of atoms as in calculations of the band structure of pure metals [18], i.e., $3d^{10}4s^1$ for copper and $3d^{9.4}4s^{0.6}$ for nickel. The lattice parameter and the radius of the muffin-tin sphere were equal to $a = 3.61594$ Å and $R_{MT} = 1.27845$ Å for copper and $a = 3.52122$ Å and $R_{MT} = 1.24495$ Å for nickel.

Calculations of the energy spectra of electrons were performed for disordered substitutional paramagnetic solid solutions over the whole concentration range at 10-at. % intervals. The total density of states $N(E)$ and partial densities of states of the components, $N_{\mathrm{Cu}}(E)$ and $N_{\mathrm{Ni}}(E)$, calculated for $Cu_{0.8}Ni_{0.2}$, $Cu_{0.6}Ni_{0.4}$, $Cu_{0.4}Ni_{0.6}$, and $Cu_{0.2}Ni_{0.8}$ alloys are shown in Figs. 1 and 2. The solid line shows the total density of states, and the dashed and dash-dotted lines show the partial densities of states. The vertical bar marks the position of the Fermi level. These figures also show the experimental $N(E)$ dependences for the alloys with close concentrations obtained by X-ray photoelectron spectros-

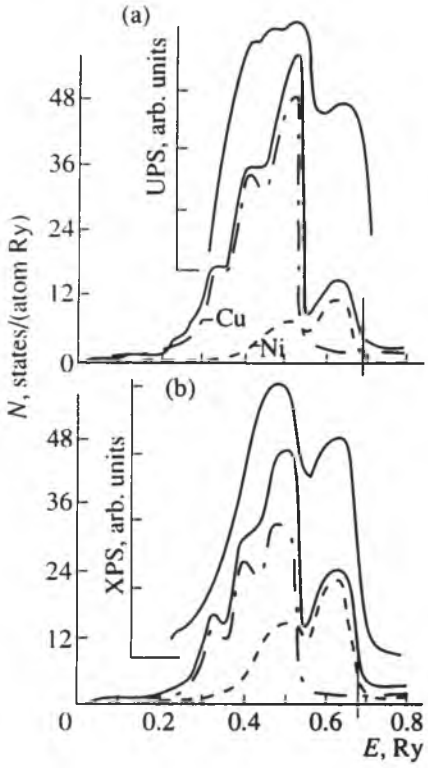

Fig. 1. Energy dependences of the total density of states (solid curve) and partial densities of states (dashed and dash–dot curves) (a) for $Cu_{0.8}Ni_{0.2}$ and (b) $Cu_{0.6}Ni_{0.4}$ alloys. The experimental UPS [23] and XPS [24] spectra are presented for nickel concentrations x = 0.23 and 0.40, respectively.

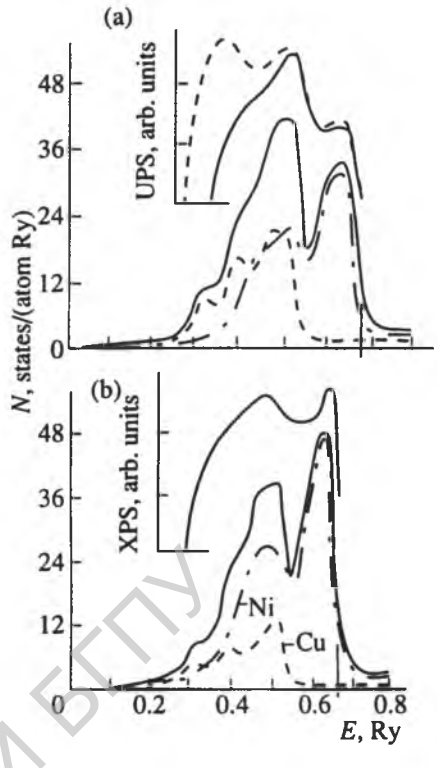

Fig. 2. Density of electron states vs. energy for (a) $Cu_{0.4}Ni_{0.6}$ and (b) $Cu_{0.2}Ni_{0.8}$. The UPS spectra are presented for the concentrations x = 0.61 and 0.81. In Fig. 2a, the UPS curves are shown for the excitation energies $h\nu$ = 9.2 eV (dashed line) and 10 eV (solid line) [23].

copy (XPS) and UV photoelectron spectroscopy (UPS) [23, 24]. These curves are shifted along the energy axis so that the Fermi levels are coincident. It is clearly seen that increasing the content of the transition component in the alloy results in an increase of the additional d peak that arises between the d band and the Fermi level of the solvent metal. The positions of copper and nickel d peaks are in good agreement with our calculation results. According to the photoemission data, the additional d peak of the alloy with 23 at. % Ni is positioned at 0.073 Ry (1.0 ± 0.05 eV) below the Fermi level of the alloy (E_F), its half-width being 0.048 Ry (0.65 ± 0.05 eV) [23]. For the nickel concentration of 20 at. %, our calculations give values 0.064 and 0.042, respectively.

The $N(E)$ dependences calculated in this paper are in close agreement with the results of self-consistent calculations for paramagnetic Cu–Ni alloys obtained by the KKR and LCAO methods and within CPA [3–6]. In Fig. 3, our $N(E)$ dependences correlate with the corresponding dependences from [3, 5, 6] for close concentrations. It is clearly seen that the relative positions and widths of d peaks given by our VCA calculations agree with the experimental data at least as closely as those obtained in the CPA or even more closely in a number of cases. As an example, we obtained for the alloy with 80% Ni that the two principal d peaks are located 0.03 and 0.18 Ry below the Fermi level; according to the photoemission data, they are positioned 0.04 and 0.20 Ry below E_F; and the calculations of [4] performed for the alloy with 81% Ni give 0.01 and 0.12 Ry. Note that in CPA calculations, the shape of the $N(E)$ curve and the relative height of the peaks are very sensitive to the scattering parameter $\delta = E_d^A - E_d^B$, which determines the energy interval between the scattering d resonances of different types of atoms, and the sensitivity is the highest for copper-rich alloys. The scattering parameter is chosen arbitrarily; in [3], e.g., it was set equal to 0.134 Ry to ensure the closest agreement between the calculated and experimental $N(E)$ curves. The δ dependence of the results is also retained in more recent developments of the KKR–CPA [4–6]. In [5], e.g., this parameter varied from 0.107 to 0.112 Ry. We calculated this interval and found it equal to 0.121 Ry.

The calculated values of the density of electron states at the Fermi level $N(E_F)$ were used for calculating

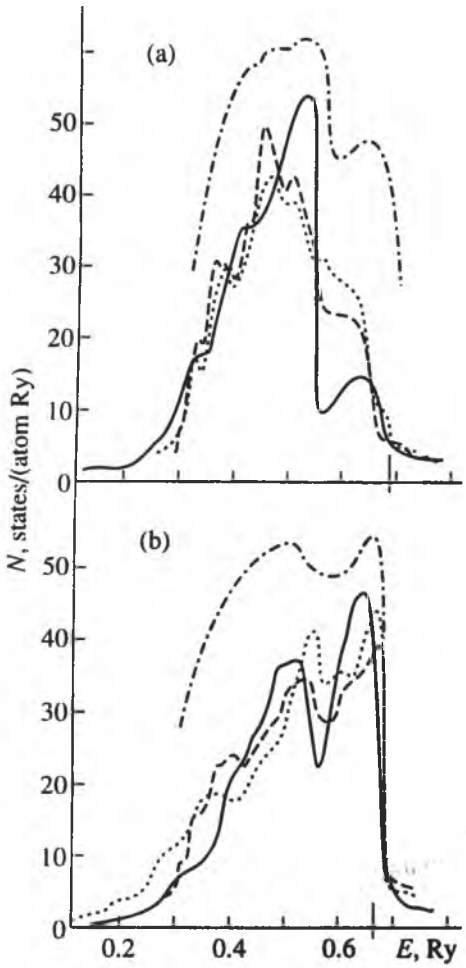

Fig. 3. Densities of electron states for (a) $Cu_{0.8}Ni_{0.2}$ and (b) $Cu_{0.2}Ni_{0.8}$ alloys calculated by different methods: solid line, our APW–VCA results; dashed line, KKR–CPA results [6]; and dash-dotted line, experimental curve [23]. The dashed curves represent (a) the results of LCAO–CPA calculations [7] and (b) the results of SCF–CPA calculations [3].

the temperature coefficient of electronic heat capacity γ via the formula

$$\gamma = \frac{\pi^2 k_B^2}{3} N(E_F)(1+\lambda), \quad (8)$$

where λ is the constant of electron–phonon interaction. For the λ constants of nickel and copper, we took the empirical values 0.3 and 0.14, respectively [21]; the $\lambda(c)$ dependence of the alloys was assumed to be linear. The calculated $\gamma(x)$ dependences are shown in Fig. 4 by filled circles (curve *4*). Figure 4 also presents the results of SCF–CPA calculations [3] with copper (curve *1*) and nickel (curve *2*) atomic configurations used as the basis. The crosses show the most recent KKR–CPA results for the heat capacity [6]. Curve *3* represents the corresponding experimental dependence obtained from measurements of low-temperature heat capacity [25]. The spike seen in curve *3* about $x = 0.5$ is associated with the transition into the ferromagnetic state. On the whole, the calculated and experimental curves are in reasonable agreement; the discrepancy, which is most pronounced near the phase transition point, is due to the fact that our results were obtained for paramagnetic alloys. Comparison of our calculation results for $\gamma(x)$ with previous results of CPA calculations [3, 4, 6] shows that the agreement with the experimental data is at least not worse for high copper contents and is even better for high nickel contents.

The absolute diffusion thermopower S was calculated via formula (4). The numerical values of total density of states at the Fermi level $N(E_F)$ are listed in the table. The derivative of the density of electron states at the Fermi level $(dN/dE)_{E=E_F}$ was calculated by approximating the $N(E_F)$ dependence with a parabola near E_F. The interval of differentiation was decreased until the derivatives to the left and to the right of E_F coincided to the fifth decimal place. The values of the

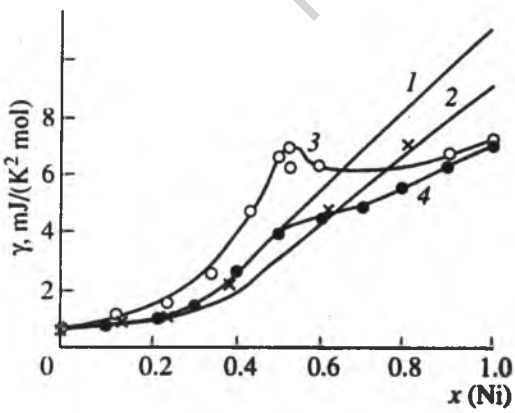

Fig. 4. Dependence of the coefficient of electronic heat capacity on nickel concentration in Cu–Ni alloys: (*1*)–(*2*) SCF–CPA calculations [3], (*3*) experimental data [25], (*4*) our calculations, and (×) KKR–CPA calculations [6].

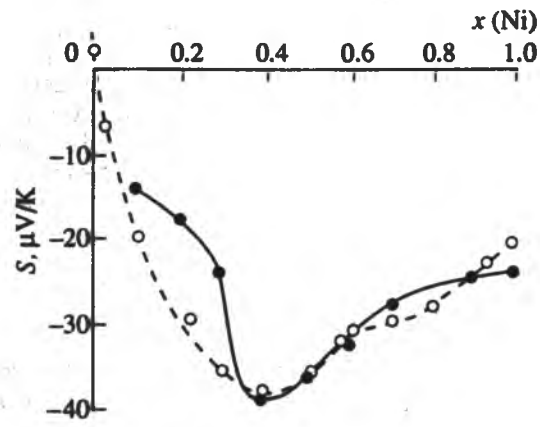

Fig. 5. Concentration dependence of the thermopower in Cu–Ni alloys: solid curve, calculated for $T = 50°C$, and dashed curve, experimental dependence measured in the temperature range of 0–100°C [2].

Calculated values of the density of electron states at the Fermi level and its derivative with respect to energy for Cu_{1-x}–Ni_x alloys

Concentration x	$N(E_F)$, states/(atom Ry)	$-(dE/dN)_{E=E_F}$, states/(atom Ry^2)
0.1	3.36	70.31
0.2	4.51	114.64
0.3	6.70	237.50
0.4	12.24	780.50
0.5	16.44	998.63
0.6	19.23	1036.56
0.7	21.70	1070.75
0.8	26.24	1122.93
0.9	29.78	1261.20
1.0	32.36	1399.47

derivatives for the selected values of concentration are listed in the table. Figure 5 shows the concentration dependence of diffusion thermopower $S(x)$ calculated for the temperature $T = 50$°C. The dashed curve in the figure shows the experimental $S(x)$ dependence for Cu–Ni alloys in the temperature range of 0–100°C borrowed from [2]. The phase transition into the ferromagnetic state is marked by a spike in the experimental curve at $x = 0.6$. The calculated $S(x)$ dependence differs slightly from the measured one; the deviation is most significant at nickel contents $x = 0.2$ and 0.3. This deviation may be a result of insufficient calculational accuracy because of non-self-consistency of the potential.

CONCLUSION

In summary, the APW-based virtual-crystal approximation provides satisfactory agreement with the experimental data (with an error equal or smaller than that of CPA) when calculating both the energy spectra and concentration dependences of the above properties of disordered paramagnetic Cu–Ni alloys in the whole range of concentrations. The qualitative agreement between the calculated results and the experimental data is achieved in the absence of adjustable or experimentally determined parameters. Hence, this is the first attempt of *ab initio* calculation of thermopower in Cu–Ni alloys in a broad concentration range.

REFERENCES

1. Mott, N.F., The Resistance and Thermoelectric Properties of the Transition Metals, *Proc. Roy. Soc. A*, 1936, vol. A156, pp. 368–382.
2. Colles, B.R., Electronic Structures and Physical Properties in the Alloy Systems Nickel–Copper and Palladium–Silver, *Proc. Phys. Soc. B*, 1952, vol. 65, pp. 221–229.
3. Stocks, G.M., Williams, R.W., and Faulkner, J.S., Density of States of Paramagnetic Cu–Ni Alloys, *Phys. Rev. B: Solid State*, 1971, vol. *B*4, no. 12, pp. 4390–4405.
4. Ehrenreich, H. and Schwartz, L., *The Electronic Structure of Alloys*, *Solid State Physics*, vol. 31, New York: Academic, 1976, pp. 149–286. Translated under the title *Elektronnaya struktura metallov*, Moscow: Mir, 1979.
5. Stocks, G.M., Temmerman, W.M., and Gyorffy, B.L., Complete Solution of the Korringa–Kohn–Rostocker Coherent-Potential Approximation Equations: Cu–Ni Alloys, *Phys. Rev. Lett.*, 1978, vol. 41, no. 5, pp. 339–343.
6. Gordon, B.E.A., Temmerman, W.M., and Gyorffy, B.L., On the Fermi Surfaces of Paramagnetic Cu_c–Ni_{1-c} Alloys, *J. Phys. F: Met. Phys.*, 1981, vol. 11, no. 4, pp. 1821–1857.
7. Richter, R., Eschrig, H., and Velicky, B., LCAO Approach to the Coherent-Potential Approximation: Electronic Structure of Substitutionally disordered CuNi Alloys, *J. Phys. F: Met. Phys.*, 1987, vol. 17, no. 2, pp. 351–372.
8. Blatt, F.J., *Physics of Electronic Conduction in Solids*, New York: McGraw-Hill, 1968.
9. Abrikosov, I.A., Vekilov, Yu.Kh., and Ruban, A.V., *Ab Initio* Calculations of Residual Resistivity and Thermopower of Copper and Aluminum Alloys, *Dokl. Akad. Nauk SSSR*, 1990, vol. 315, no. 3, pp.593–595.
10. Panin, V.E. and Fadin, V.P., The Thermopower and the Structure of the 3*d* Zone in Nickel and Its Alloys, *Philos. Mag.*, 1968, vol. 18, no. 156, pp. 1301–1304.
11. Vedernikov, M.V., Dvunitkin, V.G., and Burkov, A.T., Thermoelectric Properties of Binary Metallic Solutions with Complete Mutual Solubility, *Teplofizicheskie svoistva veshchestva: Obzory*, Moscow: Inst. Vys. Temp. Akad. Nauk SSSR, 1990, no. 5, pp. 45–92.
12. Fletcher, R. and Greig, D., The Low Temperature Thermoelectric Power of Some Palladium and Platinum Alloys, *Philos. Mag.*, 1968, vol. 17, no. 145, pp. 21–35.
13. Abel'skii, Sh.Sh., Ryzhanova, N.V., and Irkhin, Yu.P., Low-Temperature Thermopower of Pd–Ag and Pd–Au Alloys, *Fiz. Met. Metalloved.*, 1984, vol. 57, no. 2, pp. 409–410.
14. Kiang, L.L. and Lin, T.L., Thermoelectric Power of Gold–Alkali Metal Alloys, *Nuovo Cimento Lett.*, 1977, vol. 18, no. 2, pp. 41–44.
15. Butler, W.H. and Stocks, G.M., Calculated Electrical Conductivity and Thermopower of Silver–Palladium Alloys, *Phys. Rev. B: Condens. Matter*, 1984, vol. *B*29, no. 8, pp. 4217–4223.
16. Schoen, J.M., APW Virtual-Crystal Approximation, *Phys. Rev.*, 1969, vol. 184, no. 3, pp. 858–863.
17. Parmenter, R.H., Energy Levels of Disordered Alloys, *Phys. Rev.*, 1955, vol. 97, no. 3, pp. 587–598.
18. Golub, V.M. and Karolik, A.S., Non-self-consistent Calculation of Band Structure of Cu, Ni, Ag, and Pd Involving Hartree–Fock–Rothaan Wavefunctions, *Vestsi Akad. Nauk Belarusi, Ser. Fiz.-Mat. Navuk*, 1995, no. 2, pp. 87–93.
19. Lukhvich, A.A. and Karolik, A.S., Concentration Dependence of Thermoelectric Properties of Cu–Ni Alloys, *Fiz. Met. Metalloved.*, 1985, vol. 59, no. 5, pp. 1085–1090.

20. Clementi, E. and Roetti, C., Rothaan–Hartree–Fock Atomic Wavefunctions, *Atomic Data Nucl. Data Tabl.*, 1974, vol. 14, pp. 177–478.

21. Ziesche, P., Lehmann, G., Eschrig, H., Paasch, G., and Rennert. P., *Ergebnisse in der Elektronentheorie der Metallen* (Advances in the Electronic Theory of Metals), Berlin: Akademie, 1983. Translated under the title *Dostizheniya elektronnoi teorii metallov*, Moscow: Mir, 1984.

22. Nemoshkalenko, V.V. and Antonov, V.N., *Metody vychislitel'noi fiziki v teorii tverdogo tela* (Methods of Calculational Physics in Solid-State Theory), Kiev: Naukova Dumka, 1985.

23. Seib, D.H. and Spicer, W.E., Photoemission and Optical Studies of Cu–Ni Alloys: I. Cu-Rich Alloys, *Phys. Rev. B: Solid State*, 1970, vol. *B*2, no. 2, pp. 1676–1704.

24. Hufner, S., Wertheim, G., and Wernick, J., X-Ray Photoelectron Spectra of the Valence Bands of Some Transition Metals and Alloys, *Phys. Rev. B: Solid State*, 1973, vol. 8, no. 10, pp. 4511–4524.

25. Gupta, K.P., Cheng, C.H., and Beck, P., Low-Temperature Specific Heat of Ni-Based fcc Solutions with Cu, Zn, Al, Si, and Sb, *Phys. Rev. A*, 1964, vol. 133, no. 1, pp. A203–A206.